East China plains: A "basin" of ozone pollution

Chun Zhao[1], Yuhang Wang, and Tao Zeng

School of Earth and Atmospheric Science, Georgia Institute of Technology, Atlanta, GA 30332, U.S.A

Manuscript for submission to

Environmental Science and Technology

[1]Corresponding author phone: (404) 510-5331; email: chun.zhao@eas.gatech.edu

Economic growth and associated pollution emissions in China are concentrated over three connected plains to the east. We analyze an episode of highly elevated ozone over East China on June 9-14, 2004 using a 3-D chemical transport model. During this episode, the East China plains are under a high pressure system, which suppresses the ventilation of pollutants from the boundary layer. Simulated ozone concentrations over a major fraction of East China reach high levels, all the way down to the Pearl River Delta region in the southern border. The convergence of pollutant emissions and population over the vast stretch of the geographically flat plains of East China makes the region susceptible to high-ozone exposure. During this episode, the high-O_3 region extends over an area > 1 million km^2, which hosts a population of > 800 million people. Model results indicate that controlling anthropogenic NO_x emissions effectively reduces the area with high-ozone exposure.

Introduction

Ozone (O_3), an important chemical compound of the earth's atmosphere, is a greenhouse gas contributing to global warming and poses health and ecology problems on the ground level (*1*). During the past two decades, the rapid economic growth in China results in a significant increase in the emissions of ozone precursors (*2-4*) and these emissions lead to the formation of elevated ozone near the surface. In recent years, more and more observations have found high ozone episodes in China, mostly over East China (110^o-120^oE, 25^o-42^o N) (*5-9*).

East China hosts the economic engine of the country with > 60% of the industries and populations (Fig. 1a) and most of the major cities. Geographically, this region consists of

three plains: North China Plain, Northeast Plain, and Chang Jiang Downstream Plain with high mountains and plateau to the west and ocean to the east (Fig. 1b). The elevation over most of the region is less than 200 m. A similar geographical feature exists over the "South Coast Basin" of California in the United States (U.S.) (mountain regions to its east and ocean to its west). The "basin" feature contributes to high ozone episodes there (*10, 11*). As in the case of California, the East China plains also have large pollutant emissions (*3*). When the atmospheric circulation becomes favorable, widespread high ozone pollution can form over East China due to the recirculation of pollutants. Unlike the "South Coast Basin" of California, East China plains are much larger (> 1 million km^2) occupied by a larger population (> 800 million). Thus the environmental impact of ozone pollution is much greater. Unfortunately it is difficult to identify such "basin" feature of high ozone over East China since ground ozone monitoring sites in China are mostly in major cities and the measurement data are difficult to obtain for researchers outside China. In this work, we identify the "basin" feature using the simulations from a regional chemical transport model (REAM) and surface ozone measurements.

Methods

Model. The 3-D regional chemical transport model (REAM) driven by MM5 assimilated meteorological fields was described by *Choi et al.* (*12*). Previously, this model was applied to investigate a number of tropospheric chemistry and transport problems at northern mid latitudes (*13-17*) and in the polar regions (*18-20*). In this work, the REAM model is applied to ozone simulations over East Asia. The model has a horizontal resolution of 70 km with 23 vertical layers below 10 hPa. Meteorological

fields are assimilated using MM5 constrained by the National Center for Environmental Prediction (NCEP) reanalysis products. The horizontal domain of MM5 has 5 extra grids beyond that of REAM on each side to minimize potential transport anomalies near the boundary. Most meteorological field inputs are archived every 30 minutes except those related to convective transport and lightning parameterizations, which are archived every 5 minutes. Chemical initial and boundary conditions for chemical tracers in REAM are obtained from the global simulation for the same period using the GEOS-CHEM model driven by GEOS-4 assimilated meteorological fields (*21*). More detailed model description is provided in the supporting information.

Emissions. Biogenic emission algorithms and inventories are adapted from the GEOS-CHEM model (*12*). The anthropogenic emissions of tracers other than NO_x are taken from a recent bottom-up Asian emission inventory developed by *Streets et al.* for 2006 INTEX-B campaign (The detail can be obtained from http://www.cgrer.uiowa.edu/EMISSION_DATA_new/index_16.html). Anthropogenic NO_x emissions for 2004 are obtained by scaling the NO_x emissions derived by *Zhao et al.* (*22*) for 2007 over East Asia with an annual increasing rate of 8% in China (*22*). The NO_x and CO emissions from biomass burning are obtained from the Global Fire Emissions Database, Version 2 (GFEDv2.1) (*23*).

Figure 2 compares the anthropogenic NO_x emissions over China to the U.S. in 2004. The anthropogenic NO_x emission over the U.S. is prepared by Sparse Matrix Operator Kernel Emissions (SMOKE) model (http://cf.unc.edu/cep/empd/products/smoke/index.cfm) for 2004 projected from the VISTAS 2002 U.S. emission inventory. The estimated total NO_x emission over China is 6.2 Tg/yr, 35% higher than 4.6

Tg/yr over the U.S.. While high NO_x emissions are mostly over major metropolitan regions over the U.S., high NO_x emissions are more spatially spread over East China, corresponding roughly to the connected China plains shown in Figure 1b.

Results and Discussion

East China plains as a large ozone "basin". In this work, we identify the "basin" feature using the simulations from a regional chemical transport model (REAM) (*12*). Measurements from three mountain (Mt.) sites over East China, Mt. Tai (117.10^{o}E, 36.25^{o}N, 1533 m above sea level (a.s.l), center of East China), Mt. Hua (110.09^{o}E, 34.49^{o}N, 2064 m a.s.l, west edge of East China), and Mt. Huang (118.15^{o}E, 30.13^{o}N, 1836 m a.s.l, south of East China) (Fig. 1b) (*8, 24*) are used to confirm that the model simulations generally capture the observed pollution episodes. A larger episode on June 9-14 in 2004 is analyzed in this study. While the observation sites are limited, they do represent the regional feature of ozone over East China since they triangulate over the region and the sites at 1.5-2 km are high enough to avoid the influence of local pollutant emissions or distribution features. The model simulation shows high ozone concentrations (> 80 ppbv) covering the East China plains in the June episode (Fig. 1c). The meteorological condition during this episode is typical for ozone episodes, a high pressure system controlling the region, which prevents the ventilation of ozone precursors (Fig. 1d).

The ozone measurements in May at the mountain sites were previously published (*8, 24*) and were used in the model evaluation (Supporting information). The model errors for ozone simulation are within the recommended ranges of the U.S. Environmental

Protection Agency (EPA) (Supporting information). The standard model simulation shows the general characteristics of the high ozone episodes in May, but significantly underestimates some ozone peaks during the episodes at the Mt. Tai, even though it captures the general timing of the episodes.

Ozone is produced by NO_x ($NO+NO_2$) in the presence of volatile organic compounds (VOCs). The emissions of NO_x over East China used in this model are constrained by satellite measurements (Supporting information). Anthropogenic emissions of VOCs, which include a large number of species, are subject to a much higher degree of uncertainty (~130%) over Asia (*3*). Underestimation of VOCs emissions leads to underestimation of regional ozone (*25*). Our modeling analysis of observed NO, peroxyacetal nitrate (PAN), and VOCs in Beijing in August 2007 suggests that the model greatly underestimates VOCs that lead to PAN formation (unpublished results). Therefore, more VOCs are added in the model (hereafter referred to as the VOC simulation) in the form of methylglyoxal (MGLY) with the same emission distribution as propene over China. MGLY is produced from the oxidation of many VOCs and is an effective PAN precursor. In a previous model analysis, it was significantly underestimated over urban regions such as those in East China compared to limited in-situ and satellite measurements (*26*). The scaling factor of MGLY to propene emissions is determined such that PAN simulated in the model in Beijing is in agreement with the measurements. The additional MGLY emission improves the ozone simulations (next section) but its impact on the results presented in this study is limited (Supporting information).

The evaluation shows that the model performance at Mt. Tai is improved in VOC simulations, especially in producing the high ozone peaks (Supporting information). The effects at the other two mountain sites are insignificant, because ozone production in regions around these sites is sensitive to NO_x emissions whereas ozone production around Mt. Tai is sensitive to VOC emissions (next section). Therefore, we use the modeling results from the VOC simulation in this study. In the results shown, the difference between the VOC and standard simulations are small except the intensely polluted areas such as the vicinity of Beijing (Supporting information) where ozone production is sensitive to VOC emissions (next section). Due to the restriction of the agreement between two institutes in China and Japan, we were asked not to show the measurement data in June in this work. The model performance during the June episode is similar to that shown for May, and the simulated results are also better correlated with the measurements with the correlation coefficients of 0.60, 0.54, and 0.80 for Mt. Tai, Hua, and Huang, respectively.

The simulated hourly ozone concentrations at three mountain sites on June 5-16, 2004 are shown in Figure 3. Among the three mountain sites, Mt. Tai is located in an area with a high population density (Fig. 1a) and the regional emissions nearby are also higher (Fig. 2). Ozone exceeds 80 ppbv from June 9 to 14, reaching up to 120 ppbv. The VOC simulation has higher ozone concentrations than in the standard simulation especially during the high ozone episode because of ozone production sensitivity to VOCs in the surrounding area. The rapid decrease of ozone to 50 ppbv on June 15 is driven by the onset of Asian summer monsoon (*24*), when relatively clean maritime air is transported to the region. Mt. Hua is located at the western edge of the Northeast Plain. The surrounding

population and regional emissions are lower than the other two sites. As a result, the average ozone concentrations during the episode from June 9 to 14 are lower than Mt. Tai. Mt. Huang is located to the south of the Chang Jiang Downstream Plain. The model simulation shows that the episode started in the northern plains and then migrated southward. As a consequence, ozone concentrations at Mt. Huang are significantly higher on June 12-14 than the first half of the episode, reaching a maximum of ~140 ppbv, much higher than the summer average of ~45 ppbv (*24*).

We also conducted another simulation, in which anthropogenic NO_x emissions over China are removed in the model. In this sensitivity simulation, O_3 concentrations mainly reflect the transport of ozone produced in the other regions of the world and from the stratosphere and are significant lower than the standard simulation. It demonstrates that the high ozone episodes are not driven by ozone transport from the regions outside China or the stratosphere but from the ozone production inside China. The larger impact of anthropogenic NO_x emissions at Mt. Huang than Mt. Tai reflects in part ozone production sensitivity to NO_x emissions in areas around Mt. Huang, whereas ozone production around Mt. Tai is more sensitive to VOC emissions (next section). The local ozone production sensitivity is modulated by regional recirculation of ozone.

The high ozone peaks (up to 140 ppbv) at the mid night of June 14 at the three mountain sites are simulated as observed. These high ozone peaks at mid night reflect the amounts of high ozone produced photochemically on June 13 in polluted regions. The spatial distribution of the maximum daily 8-hour average (MDA8) ozone concentrations on June 13 over China from the VOC simulation is shown in Figure 1c. The ozone "basin" feature of East China is evident. The whole East China suffers from high ozone

concentrations with average MDA8 value of 93 ppbv, which normally occurs in the urban and suburban regions in the U.S. (*27*). This episode is fostered by the synoptic meteorological condition. A high pressure system locates over East China from June 11 to 13 (Fig. 1d). Under the control of the stable high pressure system which suppresses the ventilation of pollutants from the boundary layer, photochemistry produces large amounts of ozone in the polluted regions, and the meteorological condition favors the recirculation of high ozone through the connected East China plains.

Effectiveness of NO_x emissions control. Ozone production is driven mainly by NO_x and volatile organic carbons (VOCs). Photochemically, ozone production is either sensitive to NO_x emissions or to VOCs emissions. One way to diagnose the ozone production sensitivity is through the ratio of CH_2O/NO_y (*28*), where NO_y is the sum of total reactive nitrogen. The critical value determined by *Sillman et al.* (*28*) is 0.28. Above this value, ozone production is sensitive to NO_x emissions; otherwise, it is sensitive to VOC emissions. Figure 4 shows that the simulated CH_2O/NO_y ratios are > 0.6 over most regions of East China except the intensely polluted areas such as the vicinity of Beijing, indicating ozone production over a large part of East China is sensitive to NO_x emissions. Both standard and VOC simulations show similar results (Supporting information). The NO_x-sensitive region over China is consistent with *Tie et al.* (*29*) in summer. Ozone at Mt. Tai located in the VOC-sensitive region is less sensitive to NO_x emissions than at the other two mountain sites located in the NO_x-sensitive region (Fig. 3).

We apply the model to evaluate the effectiveness of reducing NO_x emissions in controlling regional ozone over East China. The changes of the MDA8 ozone concentrations from two sensitivity results (Case 1: increasing anthropogenic NO_x

emissions by 50%; Case 2: decreasing by 50%) from the VOC simulations are shown in Figure 5. Both the magnitude and the coverage of the high ozone over the East China plains on June 13 are significantly affected by the change of the NO_x emissions, since ozone production over most regions of East China are sensitive to NO_x emissions. The MDA8 ozone concentrations over East China change by +9% (an increase of 5-15 ppbv) and -16% (a decrease of 10-40 ppbv) with 50% increase and decrease of anthropogenic NO_x emissions, respectively. More sensitive to NO_x emissions than MDA8 ozone concentrations are the areas affected by high ozone concentrations. If we use the U.S. EPA MDA8 ozone standard of 75 ppbv, the areas with high ozone concentrations correspond linearly and increase or decrease by 50% from 1.3 million km^2 as the changes of the anthropogenic NO_x emissions in the model.

Satellite measurements indicate the NO_x emissions over East China have been increasing at an annual rate of 6-10% (*4, 30*). The estimated total fossil fuel NO_x emission in China is 35% higher than in the U.S. in 2004. The high emission regions in China are more widespread than in the United States. The geographically flat East China plains coupled with high anthropogenic emissions lead to high-ozone episodes, which affect > 60% of the population in China. The "basin" feature of the connected plains allows the recirculation of pollutants over the high-emission regions under high-pressure systems. Model sensitivities indicate that ozone concentrations are very responsive to NO_x emission reductions in terms of high-ozone areas and hence population exposure.

Acknowledgement

This work was supported by the National Science Foundation Atmospheric Chemistry Program.

Supporting Information Available

Supporting Information includes: 1. REAM model description; 2. Model performance evaluation using satellite NO_2 columns and surface O_3 measurements; 3. Assessment of the impact of MGLY emissions on model simulations. This information is available free of charge via the Internet at http://pubs.acs.org.

Literature Cited

(1) Intergovernmental Panel on Climate Change: IPCC FOURTH ASSESSMENTREPORT: CLIMATE CHANGE 2007. Available at http://www.ipcc.ch/ipccreports/assessments-reports.htm.

(2) Streets, D. G. and Waldhoff, S. T. Present and future emissions of air pollutants in China: SO_2, NO_x, and CO. *Atmos. Env.* **2000**, 34, 363-374.

(3) Streets, D. G.; Bond, T. C.; Carmichael, G. R.; Fernandes, S. D.; Fu, Q.; He, D.; Klimont, Z.; Nelson, S. M.; Tsai, N. Y.; Wang, M. Q.; Woo, J.-H; Yarber, K. F. An inventory of gaseous and primary aerosol emissions in Asia in the year 2000. *J. Geophy. Res.* **2003**, 108, doi:10.1029/2002JD003093.

(4) Richter, A.; Burrows, J. P.; Nub, H.; Granier, C.; Niemeier, U. Increase in tropospheric nitrogen dioxide over China observed from space. *Nature* **2005**, 437, doi:10.1038/nature04092.

(5) Lam, K. S.; Wang, T. J.; Chan, L. Y.; Wang, T.; Harris, J. Flow patterns influencing the seasonal behavior of surface ozone and carbon monoxide at a coastal site near Hong Kong. *Atmos. Env.* **2001**, 35, 3121-3135.

(6) Ma, J. and Liu, H. Summertime tropospheric ozone over China simulated with a regional chemical transport model: 1. Model description and evaluation. *J. Geophy. Res.* **2002**, 107, doi:10.1029/2001JD001354.

(7) Gao, J.; Wang, T.; Ding, A.; Liu, C. Observational study of ozone and carbon monoxide at the summit of mount Tai (1534 m a.s.l.) in central-eastern China. *Atmos. Env.* **2005**, 39, 4779-4791.

(8) Wang, Z.; Li, J.; Wang, X.; Pochanart, P.; Akimoto, H. Modeling of Regional High Ozone Episode Observed at Two Mountain Sites (Mt. Tai and Huang) in East China. *J. Atmos. Chem.* **2006**, 55, 253-272.

(9) Wang, H.; Zhou, L.; Tang, X. Ozone concentrations in rural regions of the Yangtze Delta in China. *J. Atmos. Chem.* **2006**, 54, 255-265.

(10) Altshuller, A. P. Measurements of the products of atmospheric photochemical reactions in laboratory studies and in ambient air-relationships between ozone and other products. *Atmos. Env.* **1983**, 17, 2383-2427.

(11) Kumar, S.; Chock, D. P. An update on oxidant trends in the south coarse air basin of California. *Atmos. Env.* **1984**, 18, 2131-2134.

(12) Choi, Y.; Wang, Y.; Zeng, T.; Cunnold, D.; Yang, E.; Martion, R.; Chance, K.; Thouret, V.; Edgerton, E. Springtime transitions of NO_2, CO, and O_3 over North America: Model evaluation and analysis. *J. Geophys. Res.* **2008**, 113, doi:10.1029/2007JD009632..

(13) Choi, Y.; Wang, Y.; Zeng, T.; Martin, R.; Kurosu, T. P.; Chance, K. Evidence of lightning NO_x and convective transport of pollutants in satellite observations over North America. *Geophys. Res. Lett.* **2005**, 32, doi:10.1029/2004GL021436.

(14) Choi, Y.; Wang, Y.; Yang, Q.; Cunnold, D.; Zeng, T.; Shim, C.; Luo, M.; Eldering, A.; Bucsela, E.; Gleason, J. Spring to summer northward migration of high O_3 over the western North Atlantic. *Geophys. Res. Lett.* **2008**, 35, doi:10.1029/2007GL032276.

(15) Jing, P.; Cunnold, D.; Choi, Y.; Wang, Y. Summertime tropospheric ozone columns from Aura OMI/MLS measurements versus regional model results over the United States. *Geophys. Res. Lett.* **2006**, 33, doi:10.1029/2006GL026473.

(16) Wang, Y.; Choi, Y.; Zeng, T.; Ridley, B.; Blake, N.; Blake, D.; Flocke, F. Late-spring increase of trans-Pacific pollution transport in the upper troposphere. *Geophys. Res. Lett.* **2006**, 33, doi:10.1029/2005GL024975.

(17) Guillas, S.; Bao, J.; Choi, Y.; Wang, Y. Downscaling of chemical transport ozone forecasts over Atlanta. *Atmos. Environ.* **2008**, 42, 1338-1348.

(18) Zeng, T.; Wang, Y.; Chance, K.; Browell, E. V.; Ridley, B.A.; Atlas, E. L. Widespread persistent near-surface ozone depletion at northern high latitudes in spring. *Geophys. Res. Lett.* **2003**, 30, 2298, doi:10.1029/2003GL018587.

(19) Zeng, T.; Wang, Y.; Chance, K.; Blake, N.; Blake, D.; Ridley, B. Halogen-driven low altitude O_3 and hydrocarbon losses in spring at northern high latitudes. *J. Geophys. Res.* **2006**, 111, doi:10.1029/2005JD006706.

(20) Wang, Y.; Choi, Y; Zeng, T.; Davis, D.; Buhr, M.; Huey, G.; Neff, W. Assessing the photochemical impact of snow NO_x emissions over Antarctica during ANTCI 2003. *Atmos. Environ.* **2007**, 41, 3944-3958.

(21) Bey, I.; Jacob, D. J.; Yantosca, R. M.; Logan, J. A.; Field, B.; Fiore, A. M.; Li, Q.; Liu, H.; Mickley, L. J.; Schultz, M. Global modeling of tropospheric chemistry with assimilated meteorology: Model description and evaluation. *J. Geophys. Res.* **2001**, 106, 23073-23096.

(22) Zhao, C. and Wang, Y. Daily basis inversion of NO_x emissions from OMI NO_2 columns: application for East Asia. submitted to *Geophys. Res. Lett.* **2008**.

(23) Randerson, J. T.; Van der Werf G. R.; Giglio, L.; Collatz, G. J.; Kasibhatla., P. S. Global Fire Emissions Database, Version 2 (GFEDv2.1). Available at http://daac.ornl.gov/ from Oak Ridge National Laboratory Distributed Active Archive Center, Oak Ridge, Tennesse, U.S.A. doi:10.3334/ORNLDAAC/849.

(24) Li, J.; Wang, Z.; Akimoto, H.; Gao, C.; Pochanart, P.; Wang, X. Modeling study of ozone seasonal cycle in lower troposphere over East Asia. *J. Geophy. Res.* **2007**, 112, doi:10.1029/2006JD008209.

(25) Wang, Y.; Jacob, D. J.; Logan, J. A. Global simulation of tropospheric O_3-NO_x-hydrocarbon chemistry. 3. Origin of tropospheric ozone and effects of non-methane hydrocarbons. *J. Geophys. Res.* **1998**, 103, 10757-10768.

(26) Fu, T.-M.; Jacob, D. J.; Wittrock, F.; Burrows, J. P.; Vrekoussis, M. Global budgets of atmospheric glyoxal and methylglyoxal, and implications for formation of secondary organic aerosols. *J. Geophys. Res.* **2008**, 113, D15303.

(27) North American Research Strategy for Tropospheric Ozone (NARSTO), *An Assessment of Tropospheric Ozone Pollution - A North American Perspective* (2000). Available at http://www.narsto.org/section.src?SID=7.

(28) Sillmam, S. The use of NO_y, H_2O_2, and HNO_3 as indicators for ozone-NOx-hydrocarbon sensitivity in urban locations. *J. Geophys. Res.* **1995**, 100, 14175-14188.

(29) Tie, X.; Chandra, S.; Ziemke, J. R.; Granier, C.; Brasseur, G. P. Satellite Measurements of Tropospheric Column O_3 and NO_2 in Eastern and Southeastern Asia: Comparison with a Global Model (MOZART-2). *J. Atmos. Chem.* **2007**, 56, 105-125.

(30) Zhang, Q.; Streets, D. G.; Kebin, H.; Wang, Y.; Richter, A.; Burrows, J. P.; Uno, I.; Jang, C. J.; Chen, D.; Yao, Z.; Lei, Y. NO_x emission trends for China, 1995-2004: The view from the ground and the view from space. *J. Geophys. Res.* **2007**, 112, doi:10.1029/2007JD008684.

Figure Captions:

Figure 1. (a) Distribution of provincial population density in China in 2000; (b) Terrain height distribution over East Asia with a 5-km resolution. The red square, diamond, and triangle symbols represent the locations of Mt. Tai, Hua, and Huang, respectively; (c) Ground-level MDA8 ozone concentrations over East Asia on June 13 in 2004 from the VOC simulation; (d) Simulated 700-hPa geopotential height distribution on June 13.

Figure 2. Distributions of anthropogenic NO_x emissions over China (left) and the United States (right) in 2004.

Figure 3. Simulated hourly O_3 concentrations on June 5-16 in 2004 at three mountain sites (top to bottom: Mt. Tai, Hua, and Huang). Five model results are shown: the standard simulation (black line), three VOC simulations (standard - solid orange line, 50% increase of Chinese NO_x emissions - dotted orange line, and 50% decrease of Chinese NO_x emissions – dashed orange line), and the simulation without anthropogenic NO_x emissions over China (blue line).

Figure 4. REAM simulated mean daytime ratios of CH_2O/NO_y for June 2004 over China in the VOC simulation. The black square, diamond, and triangle symbols represent the locations of Mt. Tai, Hua, and Huang, respectively.

Figure 5. Ground-level MDA8 O_3 concentrations over East Asia on June 13 in 2004 from the VOC simulations by increasing (Case 1) or decreasing (Case 2) the anthropogenic NO_x emissions over China by 50%.

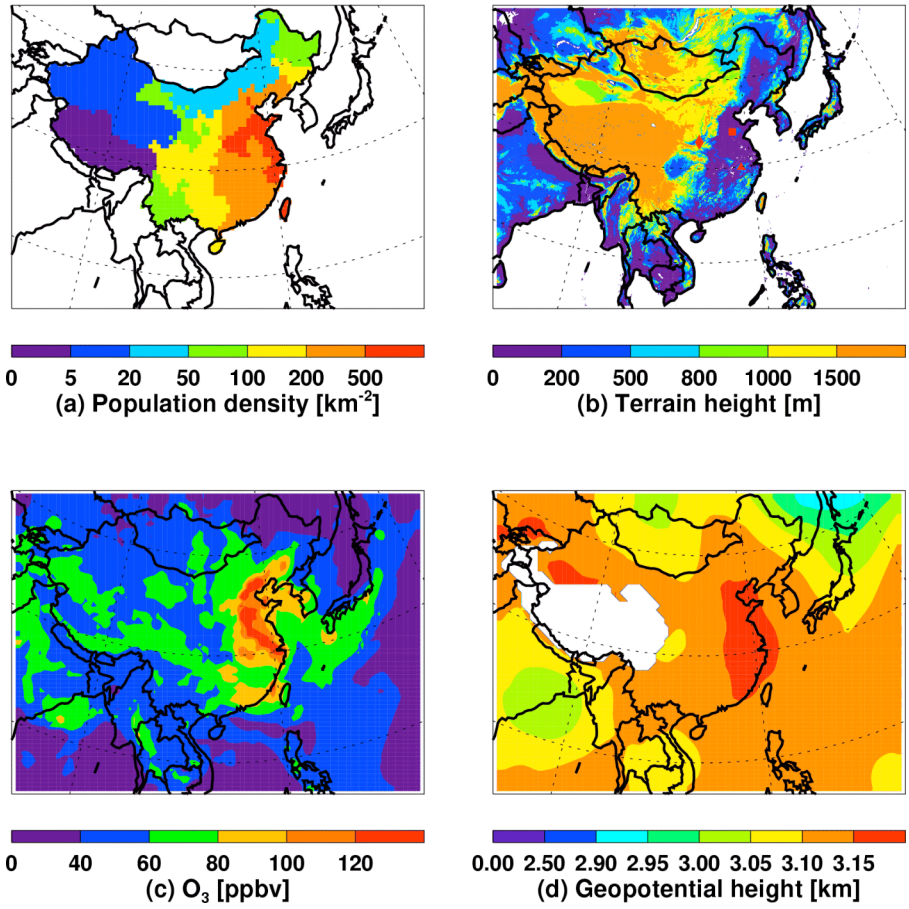

Figure 1. (a) Distribution of provincial population density in China in 2000; (b) Terrain height distribution over East Asia with a 5-km resolution. The red square, diamond, and triangle symbols represent the locations of Mt. Tai, Hua, and Huang, respectively; (c) Ground-level MDA8 ozone concentrations over East Asia on June 13 in 2004 from the VOC simulation; (d) Simulated 700-hPa geopotential height distribution on June 13.

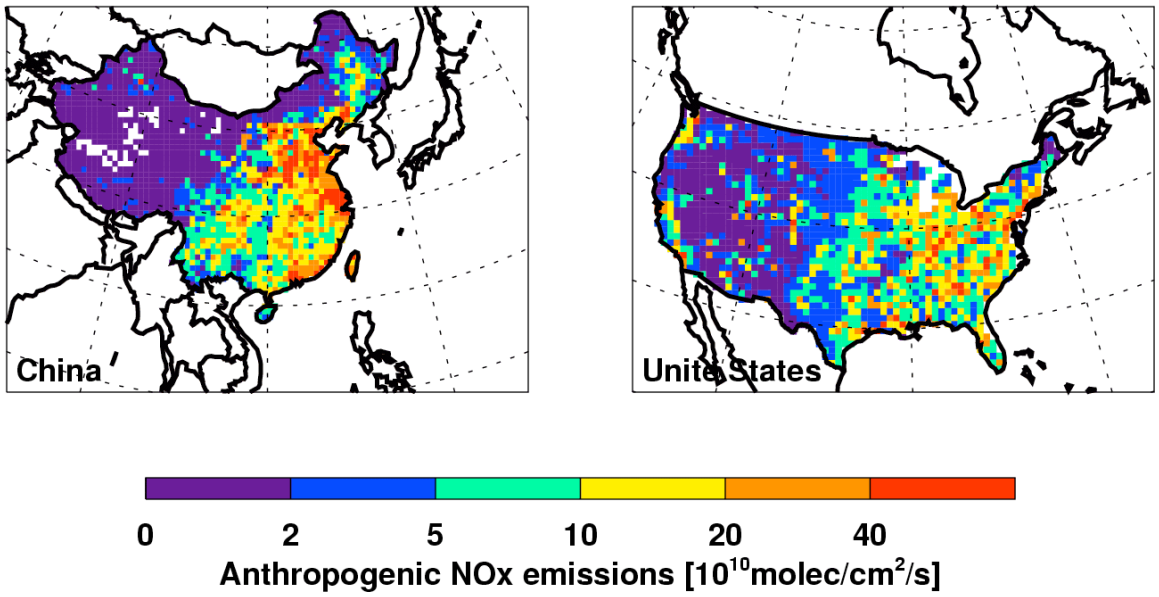

Figure 2. Distributions of anthropogenic NO_x emissions over China (left) and the United States (right) in 2004.

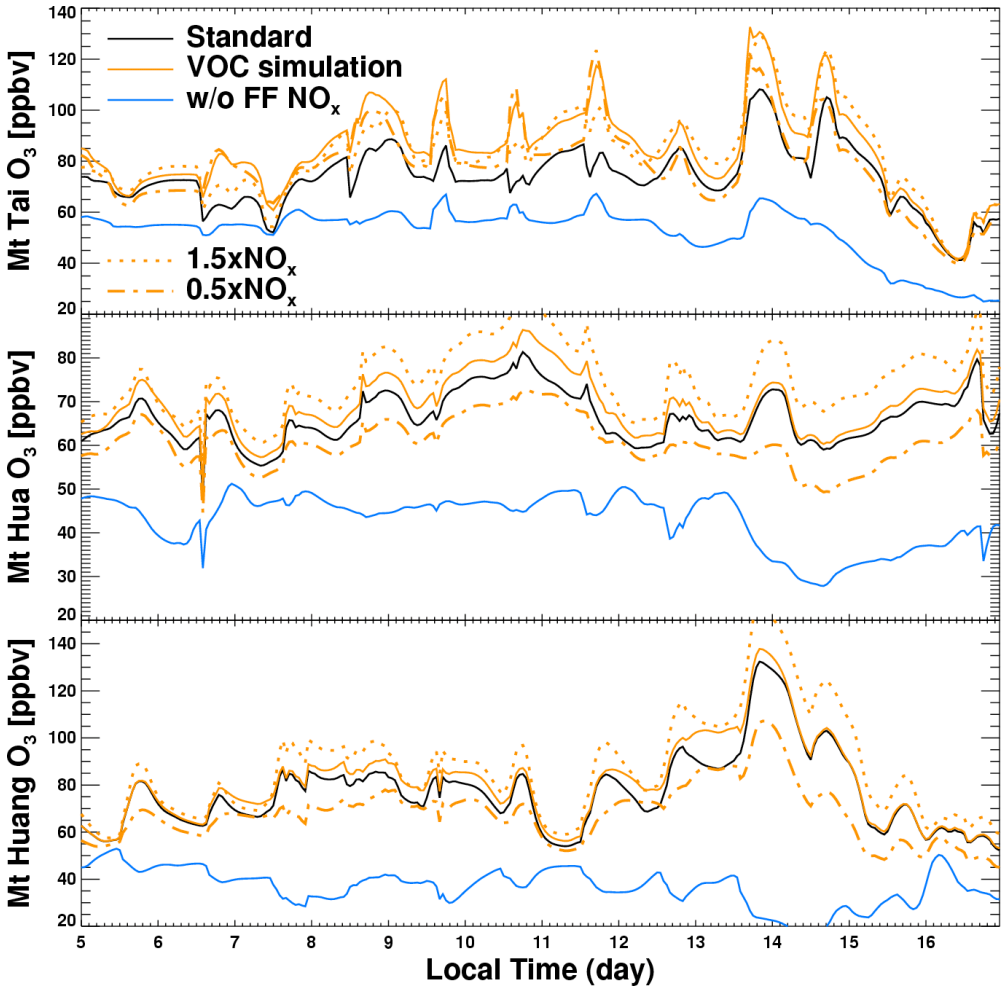

Figure 3. Simulated hourly O_3 concentrations on June 5-16 in 2004 at three mountain sites (top to bottom: Mt. Tai, Hua, and Huang). Five model results are shown: the standard simulation (black line), three VOC simulations (standard - solid orange line, 50% increase of Chinese NO_x emissions - dotted orange line, and 50% decrease of Chinese NO_x emissions – dashed orange line), and the simulation without anthropogenic NO_x emissions over China (blue line).

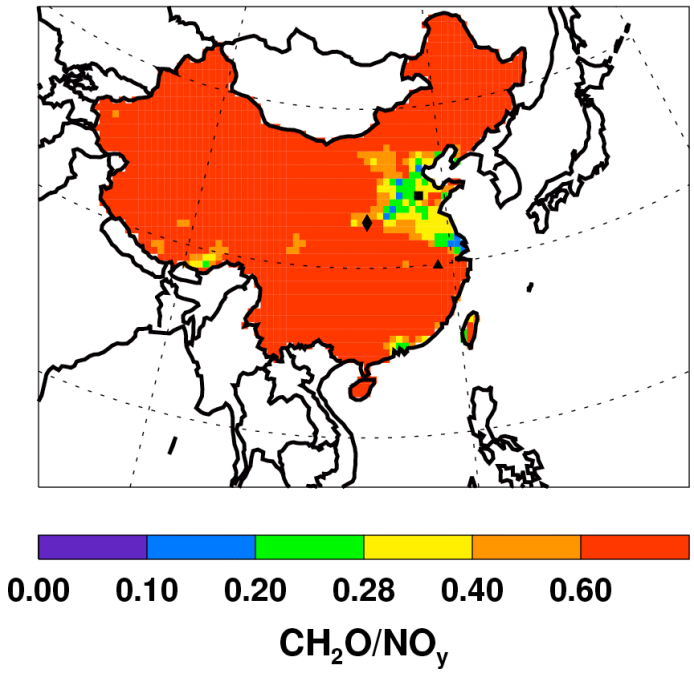

Figure 4. REAM simulated mean daytime ratios of CH_2O/NO_y for June 2004 over China in the VOC simulation. The black square, diamond, and triangle symbols represent the locations of Mt. Tai, Hua, and Huang, respectively.

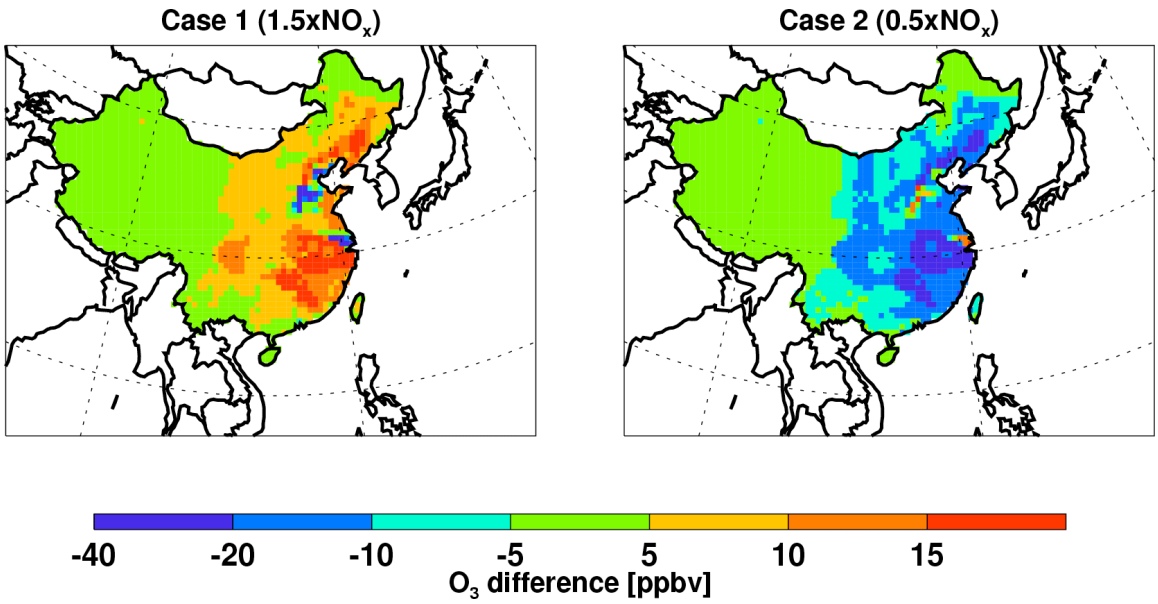

Figure 5. Changes of ground-level MDA8 O_3 concentrations over China on June 13 in 2004 from the VOC simulations by increasing (Case 1) or decreasing (Case 2) the anthropogenic NO_x emissions over China by 50%.

Table of Contents brief:

In this work, we investigate the "basin"-like feature of ozone pollution over China at a scale not seen in the other countries of the world and its implication for air pollution control.

Supporting information

East China plains: A "basin" of ozone pollution

Chun Zhao[1], Yuhang Wang, and Tao Zeng

School of Earth and Atmospheric Science, Georgia Institute of Technology, Atlanta, GA 30332, U.S.A

[1]Corresponding author phone: (404) 510-5331; email: chun.zhao@eas.gatech.edu

Number of pages: 8

Number of tables: 1

Number of figures: 3

1. REAM model description

In this work, the REAM model has a horizontal resolution of 70 km with 23 vertical layers reaching 10 hPa, 20 of which are below 100 hPa. The National Center of Atmospheric Research/Penn State MM5 is used to simulate meteorological fields using four-dimensional data assimilation (FDDA) (*S1*). The photochemistry module and the algorithms for dry and wet deposition and emissions from vegetation and soils are adopted from the GEOS-CHEM model (*S2*). The altitude-dependent cloud optical depth is calculated using MM5 liquid water content (*S3*). The UV surface albedo distribution, for photolysis rate calculations, is obtained from TOMS observations (*S4*). The transport scheme is by *Walcek* (*S5*). The convection scheme by *Grell* (*S6*) is implemented to be consistent with the meteorological model. The lightning NO_x emission is parameterized by *Choi et al.* (*S7*). Twenty-four chemical tracers describing tropospheric O_3 chemistry (*S2*) were transported.

2. REAM model evaluations

2.1. Tropospheric NO_2 columns

The tropospheric NO_2 columns retrieved from the OMI instrument (*S8*) onboard the NASA Aura satellite are used to confirm that the anthropogenic NO_x emissions in the model do not have significant biases. As the OMI tropospheric NO_2 columns are not available for June 2004, we evaluate the emissions for June 2005 (scaled from the emissions for June 2004 with 8% increasing rate). The retrieved tropospheric NO_2 columns and its uncertainties are obtained as by *Zhao et al*. (*S9*) from two independent products: near-real time (NRT) tropospheric NO_2 columns retrieved by KNMI/NASA

(*S10*) and OMI standard product at NASA Goddard Earth Sciences Data and Information Services Center (GES-DISC) (*S8*). We obtain the "best-estimates" of tropospheric NO_2 columns by averaging the columns from KNMI and GES-DISC weighted by their uncertainties. We use two methods to estimate the errors in the combined OMI columns. The first method is to estimate the errors as the root mean square of the uncertainties of the two retrievals. The second method is to estimate the error as the deviations of KNMI and GES-DISC retrievals from their means. We take the larger of the two estimates as the uncertainty for the combined OMI columns, which is around 40% over the polluted regions and reaches a factor of 1.5 over the ocean and clean continent such as western China. Only the OMI tropospheric NO_2 column data with cloud fractions of < 30% are used in the study. The comparison is shown in Figure S1. The model successfully reproduces the satellite measurements, and the mean bias and correlation coefficient between simulated and observed tropospheric NO_2 columns over China is 0.25×10^{15} molecules/cm^2 (~10%) and 0.89 respectively. The model bias is within the uncertainty of satellite measurements.

2.2. Ozone

Hourly ozone observations at Mt. Tai and Huang in May 2004 are compared to the REAM simulation results (Fig. S2). The data at Mt. Hua are not available for May 2004. The standard model generally captures the high ozone concentrations, and the correlation coefficients between the simulation and measurements are 0.49 and 0.53 for Mt. Tai and Huang respectively. The VOC simulation at Mt. Tai improves the comparison, and the correlation coefficient increases to 0.59. The VOC simulation does not significantly change the simulation at Mt. Huang, so only the standard simulation results are shown.

Three statistical measures recommended by the U.S. EPA (*S11*) are used here, Mean Normalized Bias (MNB), Mean Normalized Gross Error (MNGE), and Average Peak Prediction Accuracy (APPA) (Table S1). The REAM model errors for ozone simulations are within the EPA recommended criteria of ±15, ±30, and ±20% for MNB, MNGE, and APPA, respectively. Model shows good performance in simulating the ozone peaks during the episodes. The standard model tends to have a low bias at Mt. Tai. The VOC simulation improves the model performance at Mt. Tai. The mean bias is reduced from -4.82 to 0.03 ppbv and the APPA is improved from -15.59% to -6.58%.

3. Assessment of the impact of MGLY emissions on model simulations

Figure S3a shows the difference of simulated surface MDA8 O_3 concentrations over China between the VOC and standard simulations for June 9-14, 2004. The change of the ozone concentration over the most regions of East China is < 10 ppbv, except for the VOC-sensitive areas such as the vicinity of Beijing where the ozone enhancement reaches 10-15 ppbv. Among the three mountain sites, only Mt. Tai locates in the regions with ozone enhancement of 10-15 ppbv. Figure S3b shows the simulated mean daytime ratios of CH_2O/NO_y for June 2004 over China in the standard simulation, which is similar to the VOC simulation result (Fig. 4).

Literature Cited

(S1) Stauffer, D. R.; Seaman, N. L.; Binkowski, F. S. Use of four-dimensional data assimilation in a limited-area mesoscale model part II: effects of data assimilation within the planetary boundary layer. Mon. Weather Rev. **1991**, 119, 734-754.

(S2) Bey, I.; Jacob, D. J.; Yantosca, R. M.; Logan, J. A.; Field, B.; Fiore, A. M.; Li, Q.; Liu, H.; Mickley, L. J.; Schultz, M. Global modeling of tropospheric chemistry with assimilated meteorology: Model description and evaluation. *J. Geophys. Res.* **2001**, 106, 23073-23096.

(S3) Stephens, G. L.; Paltridge, G. W.; Platt, C. M. R. Radiation profiles in extended water clouds III: observations. *J. Atmos. Sci.* **1978**, 35, 2133-2141.

(S4) Herman, J. R. and Celarier, E. A. Earth surface reflectivity climatology at 340-380 nm from TOMS data, *J. Geophys. Res.* **1997**, 102, 28003-28011.

(S5) Walcek, C. J. Minor flux adjustment near mixing ratio extremes for simplified yet highly accurate monotonic calculation of tracer advection. *J. Geophys. Res.* **2000**, 105, 9335-9348.

(S6) Grell, G. A. Prognostic evaluation of assumptions used by cumulus parameterizations. *Mon. Weather Rev.* **1993**, 121, 764-787.

(S7) Choi, Y.; Wang, Y.; Zeng, T.; Martin, R.; Kurosu, T.; Chance, K. Evidence of lightning NO_x and convective transport of pollutants in satellite observations over North America. *Geophys. Res. Lett.* **2005**, 32, L02805.

(S8) Bucsela, E. J.; Celarier, E. A.; Wenig, M. O.; Gleason, J. F.; Veefkind, J. P.; Boersma, K. F.; Brinksma, E. J. Algorithm for NO_2 vertical Column Retrieval From the Ozone Monitoring Instrument. *IEEE Trans. Geo. Rem. Sens.* **2006**, 44(5), 1245-1258, Special Issue on the EOS Aura Mission.

(S9) Zhao, C. and Wang, Y. Daily basis inversion of NO_x emissions from OMI NO_2 columns: application for East Asia. submitted to *Geophys. Res. Lett.* **2008**.

(S10) Boersma, K. F.; Eskes, H. J.; Veefkind, J. P.; Brinksma, E. J.; Van der R. J.; Sneep, M.; Van den G. H. J.; Levelt, P. F.; Stammes, P.; Gleason, J. F.; Bucsela, E. J. Near-real time retrieval of tropospheric NO_2 from OMI, *Atmos. Chem. Phys.* **2007**, 7, 2103-2118.

(S11) U.S. EPA, *Analysis in attainment demonstrations for guidance on the use of models and other the 8-hour ozone NAAQS*. Draft Final Report, EPA-454/R-99-004, **2005**.

(S12) Wang, Z.; Li, J.; Wang, X.; Pochanart, P.; Akimoto, H. Modeling of Regional High Ozone Episode Observed at Two Mountain Sites (Mt. Tai and Huang) in East China. *J. Atmos. Chem.* **2006**, 55, 253-272.

Tables and figures:

Table S1. Statistics of model performance evaluation for hourly ozone for May 2004

		N_Obs[1]	Obs_Mean[1] (ppbv)	Sim_Mean[1] (ppbv)	Mean_Bias[1] (ppbv)	Mean_Error[1] (ppbv)	R[1]	MNB %	MNGE %	APPA %
Mt.Tai	VOC[2]	648	63.74	63.77	0.03	11.41	0.59	4.44	19.96	-6.58
	STD[2]			58.93	-4.82	12.53	0.49	-3.13	20.39	-15.59
Mt.Huang	VOC	648	63.99	66.52	2.53	12.85	0.53	8.48	21.15	2.99
	STD			66.02	2.01	12.65	0.53	7.49	20.60	2.40

[1.] N_Obs denotes the number of observations. Obs_Mean denotes the observed mean. Sim_Mean denotes the simulated mean. Mean_Bias denotes the mean of the bias of the model simulations. Mean_Error denotes the mean of the absolute bias of the model simulations. R denotes the correlation coefficient.

[2.] VOC denotes the VOC simulations. STD denotes the standard simulations.

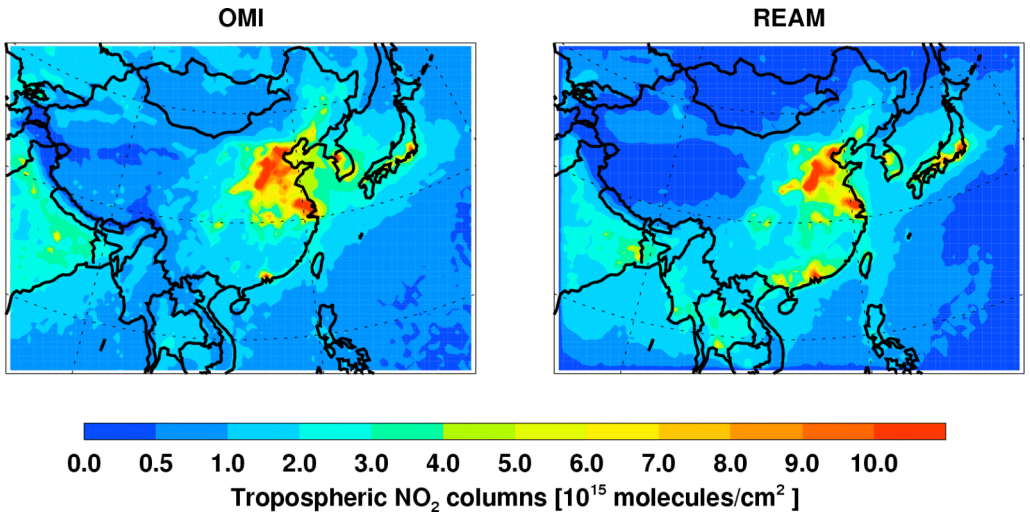

Figure S1. Monthly mean tropospheric NO_2 columns over East Asia for June 2005 from OMI measurements (left), and the corresponding REAM results. Only OMI data with cloud fractions of < 30% are used.

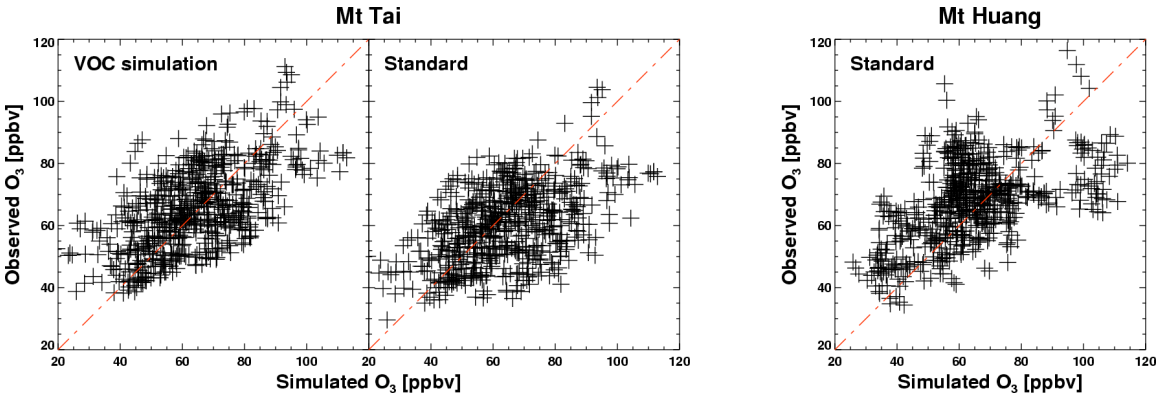

Figure S2. Observed and simulated hourly ozone concentrations from the measurements and REAM simulations at Mt. Tai and Huang for May 2004. Simulated ozone concentrations in the VOC simulation at Mt. Huang are similar to the standard simulation. The ozone measurements were previously published by *Wang et al.* (*S12*).

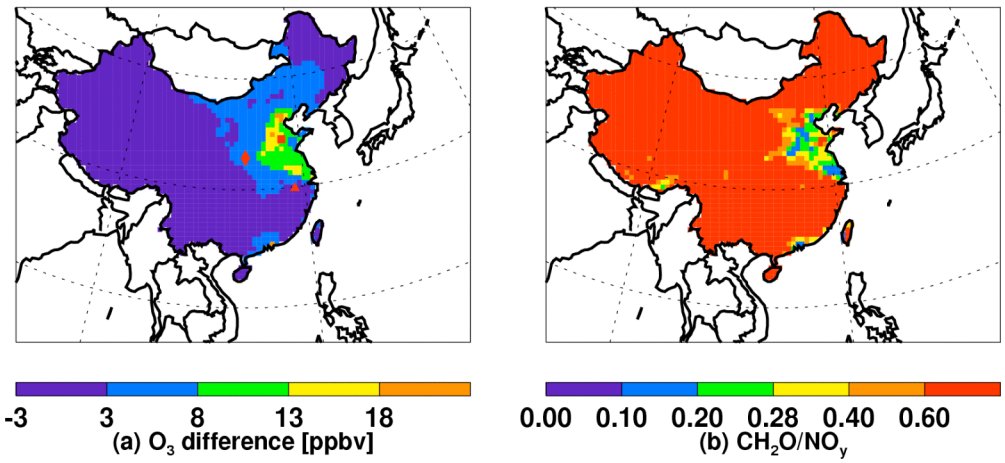

Figure S3. (a) Changes of surface MDA8 O_3 concentrations over China for June 9-14, 2004 due to the added MGLY emissions. The red square, diamond, and triangle symbols represent the locations of Mt. Tai, Hua, and Huang, respectively. (b) Simulated mean daytime ratios of CH_2O/NO_y for June 2004 over China in the standard simulation.